Supporting Information

Self-isomerised-cyclometallated rhodium NHC complexes as active catalysts in the hydrosilylation of internal alkynes

Estefan van Vuuren,[a] Frederick P. Malan,[a] Werner Cordier,[b] Margo Nell[b] and Marilé Landman[a]*

[a]*Department of Chemistry, University of Pretoria, Hatfield, Pretoria, South Africa, 0002*
[b]*Department of Pharmacology, University of Pretoria, Arcadia, Pretoria, South Africa, 0007*

Email: marile.landman@up.ac.za

1. ^{1}H, ^{13}C, and selected 2D (HSQC, COSY) NMR spectra of the rhodium complexes (**Figures S1-S20**).
2. ^{1}H NMR spectra of the Ag- and Rh-carbene intermediate species (**Figures S21**, **S22**).
3. Crystallographic data and structure refinement parameters (**Tables S1-S3**).
4. ^{1}H NMR spectra of the catalysis reaction mixtures obtained in C_6D_6 (**Figures S23-S25**).
5. Conversion *versus* time plot using **2** (**Figure S26**).
6. Proposed mechanism for the catalytic hydrosilylation of alkynes using the N-bound Rh complexes as pre-catalysts (**Scheme S1**).

1. ^{1}H, ^{13}C, and selected 2D (HSQC, COSY) NMR spectra of the rhodium complexes (**Figures S1-S20**).

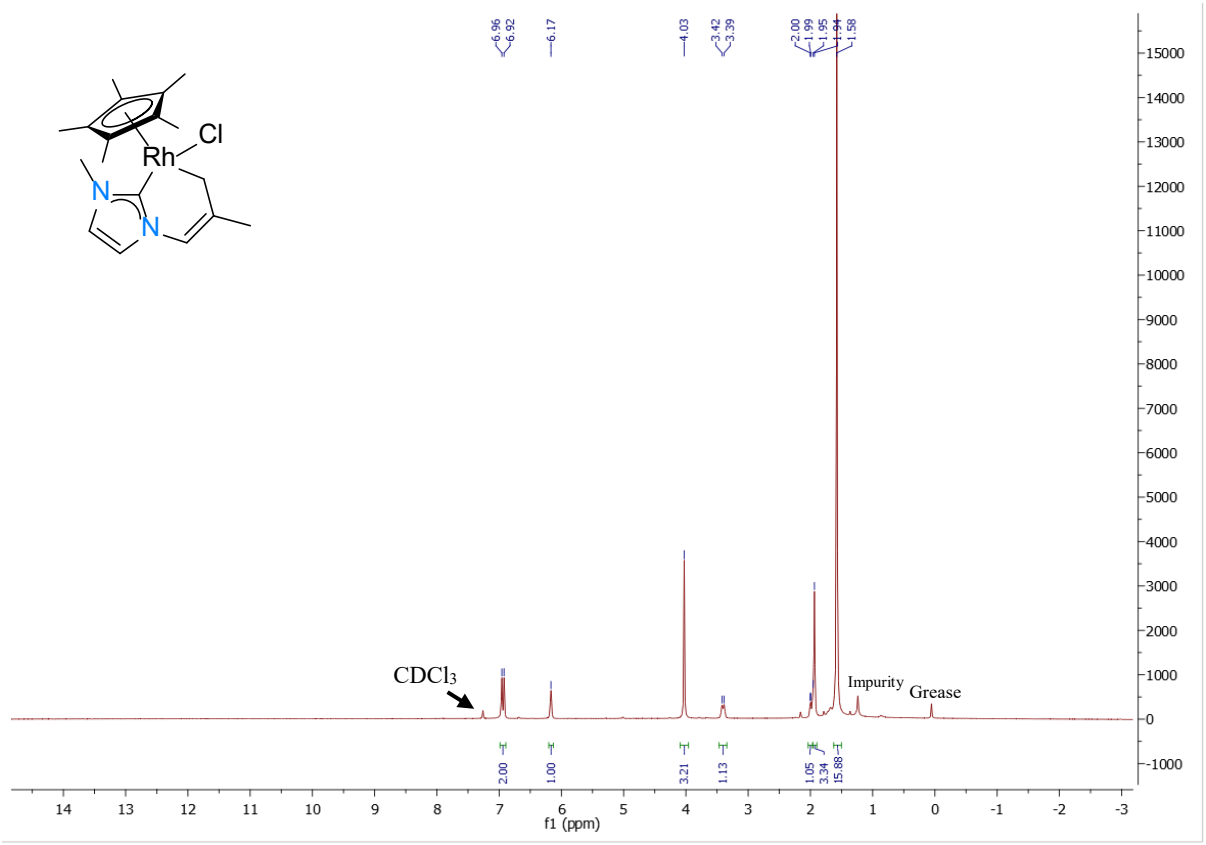

Figure S1 ^{1}H NMR spectrum of complex **1**.

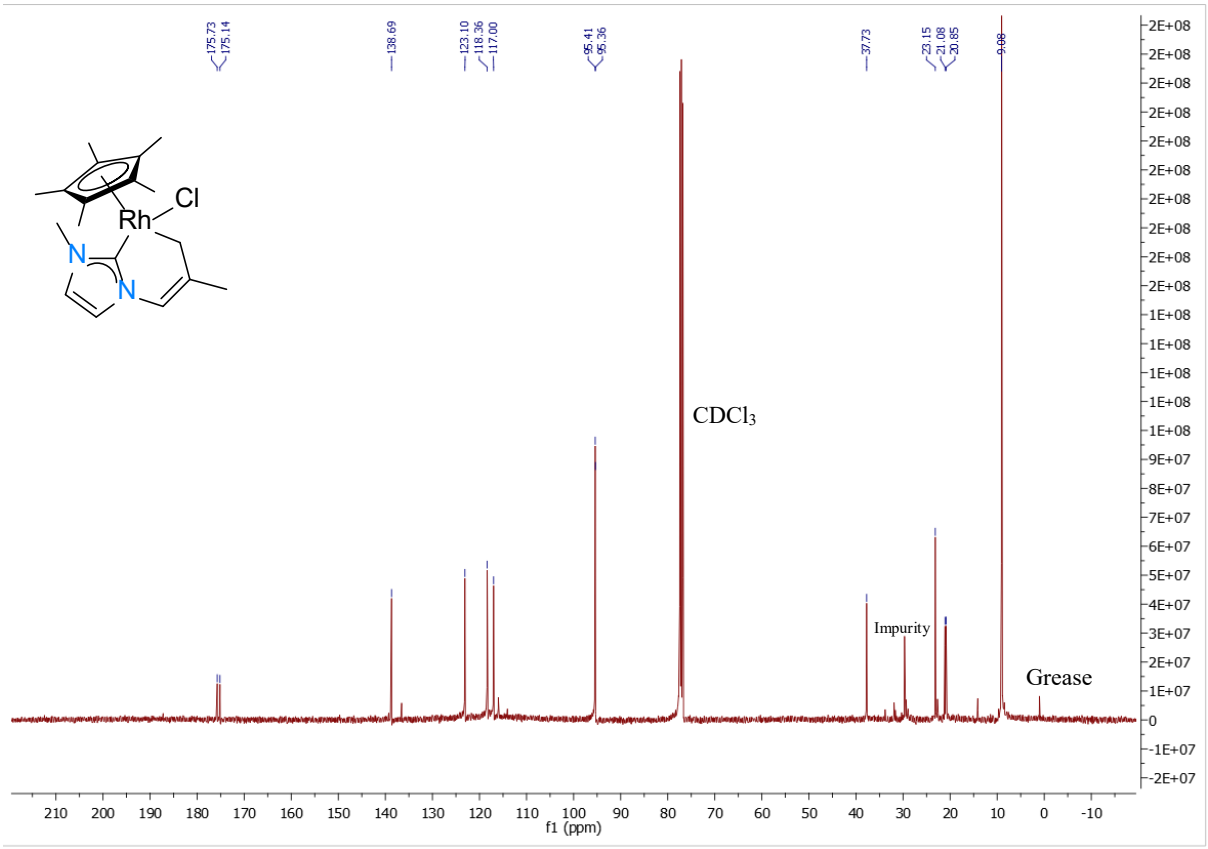

Figure S2 ^{13}C NMR spectrum of complex **1**.

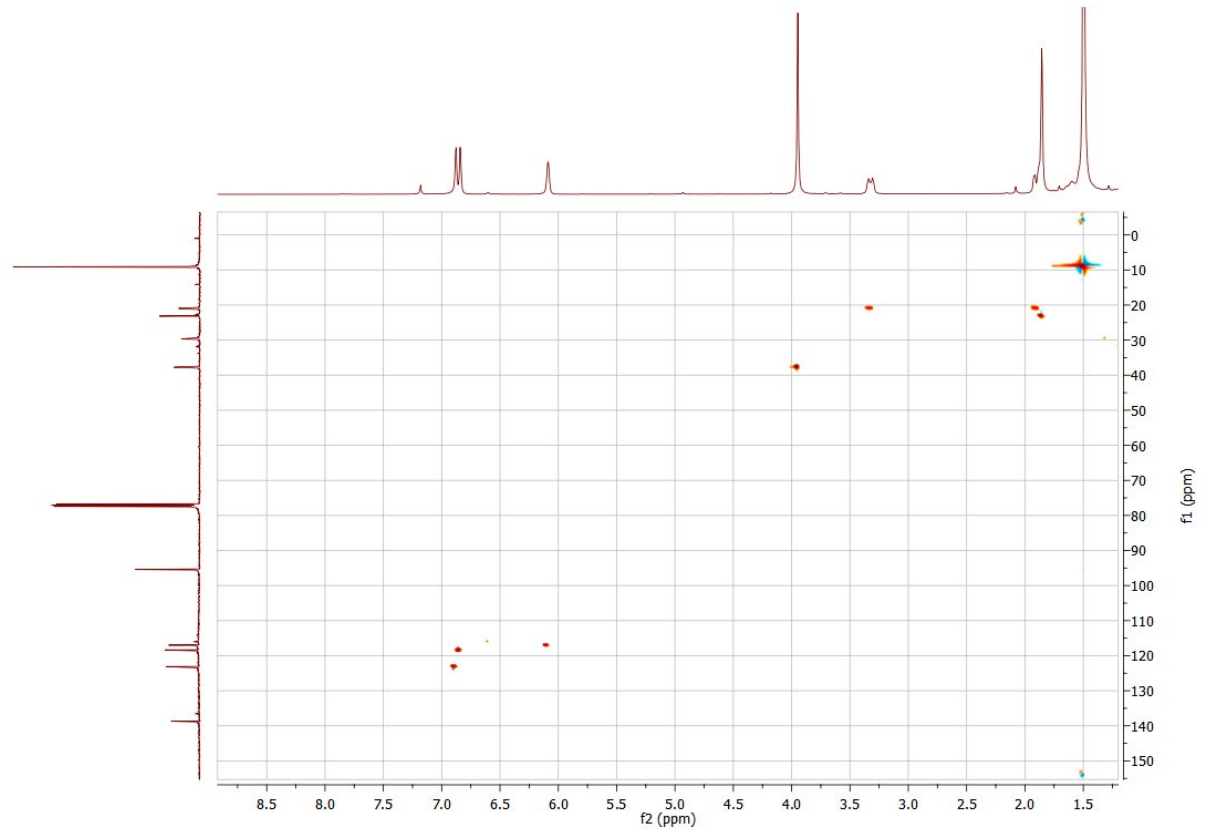

Figure S3 2D-HSQC $^{13}C\{^{1}H\}$ NMR spectrum of complex **1**.

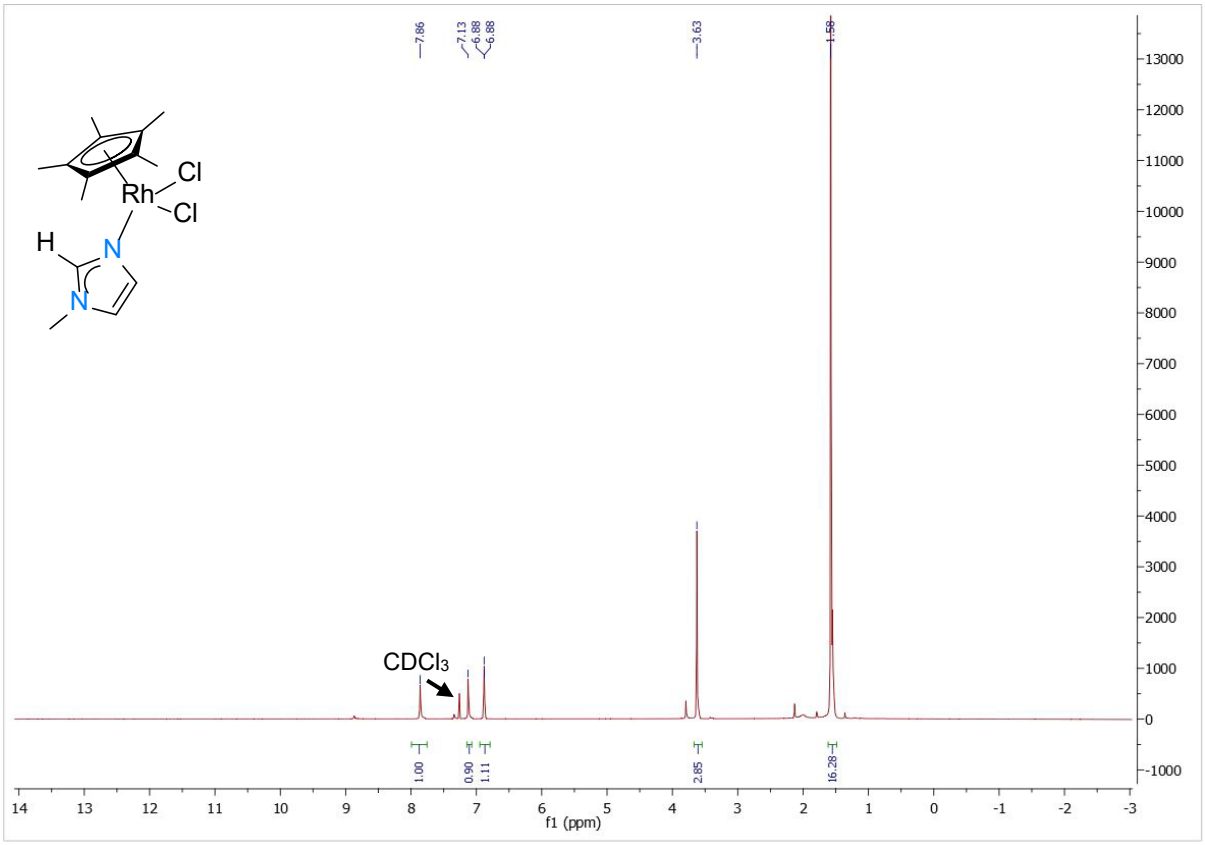

Figure S4 ^{1}H NMR spectrum of complex **1b**.

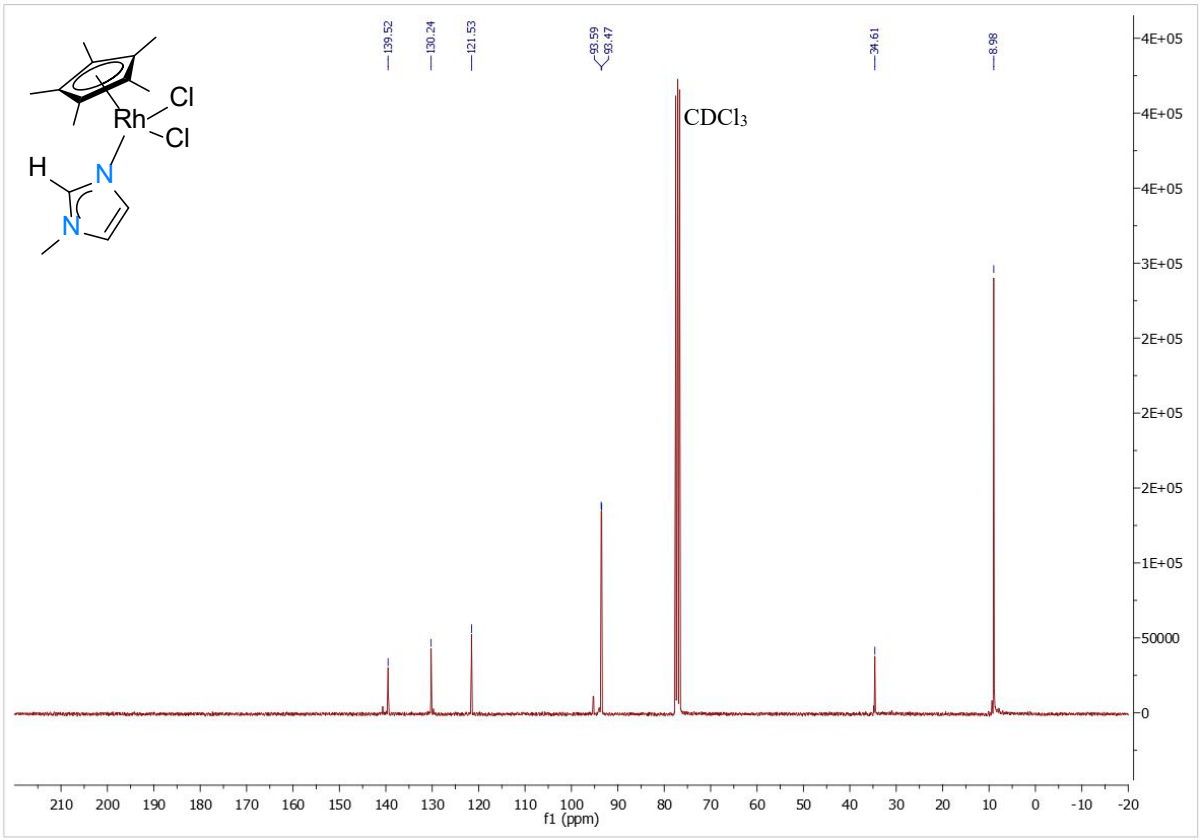

Figure S5 ^{13}C NMR spectrum of complex **1b**.

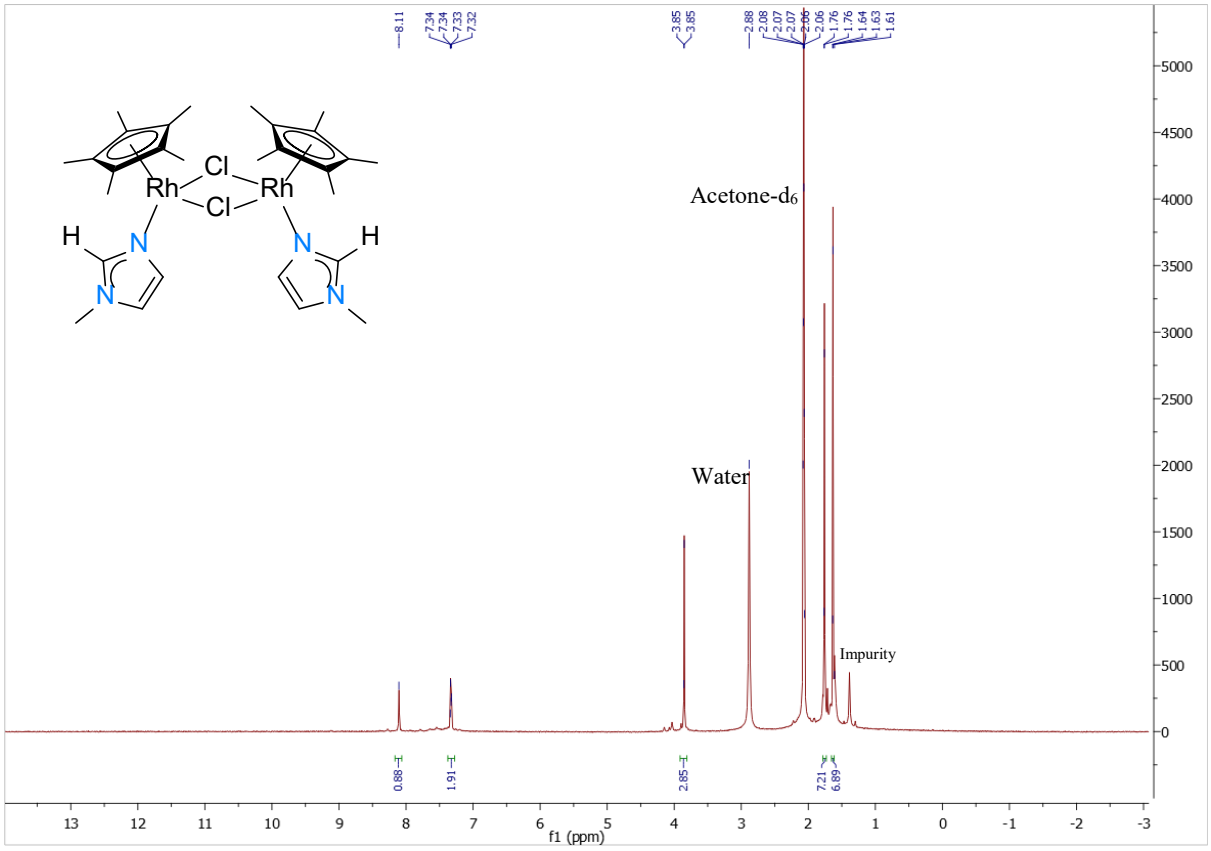

Figure S6 ^{1}H NMR spectrum of complex **1bd**.

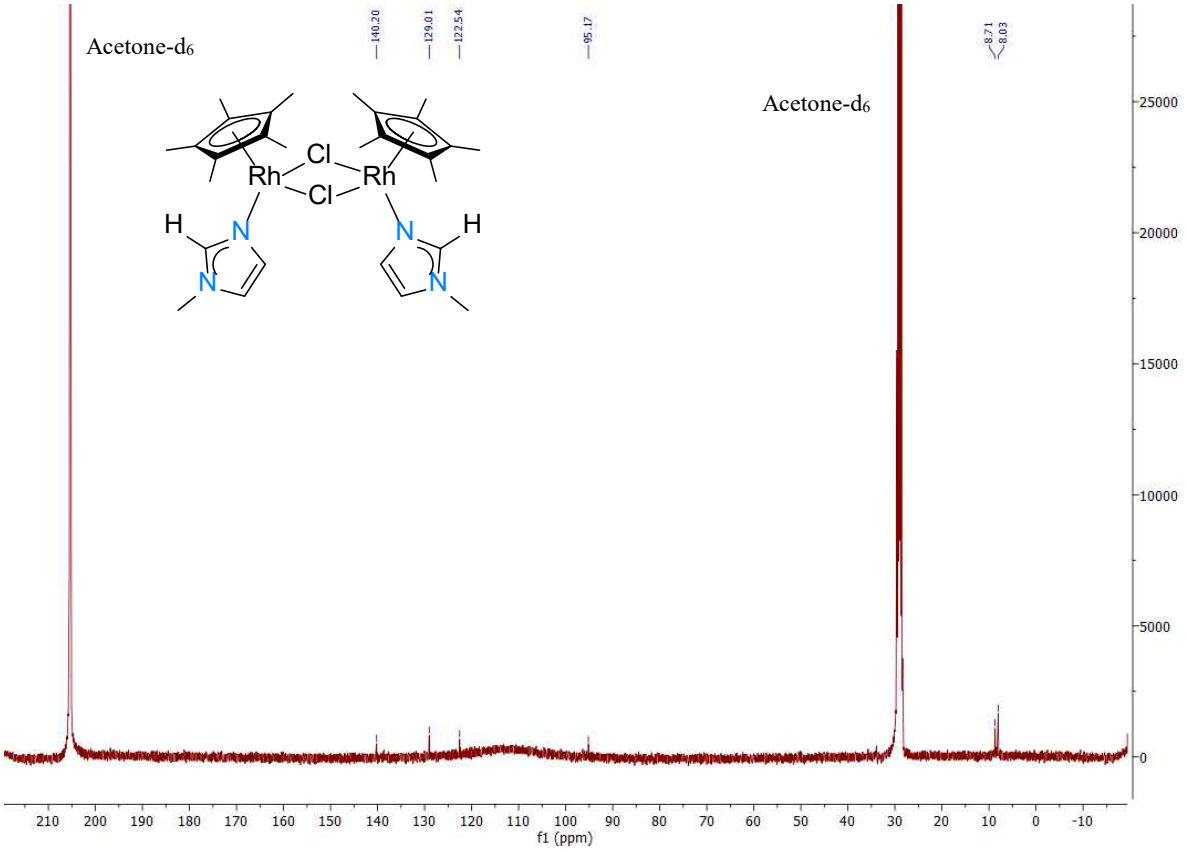

Figure S7 ^{13}C NMR spectrum of complex **1bd**.

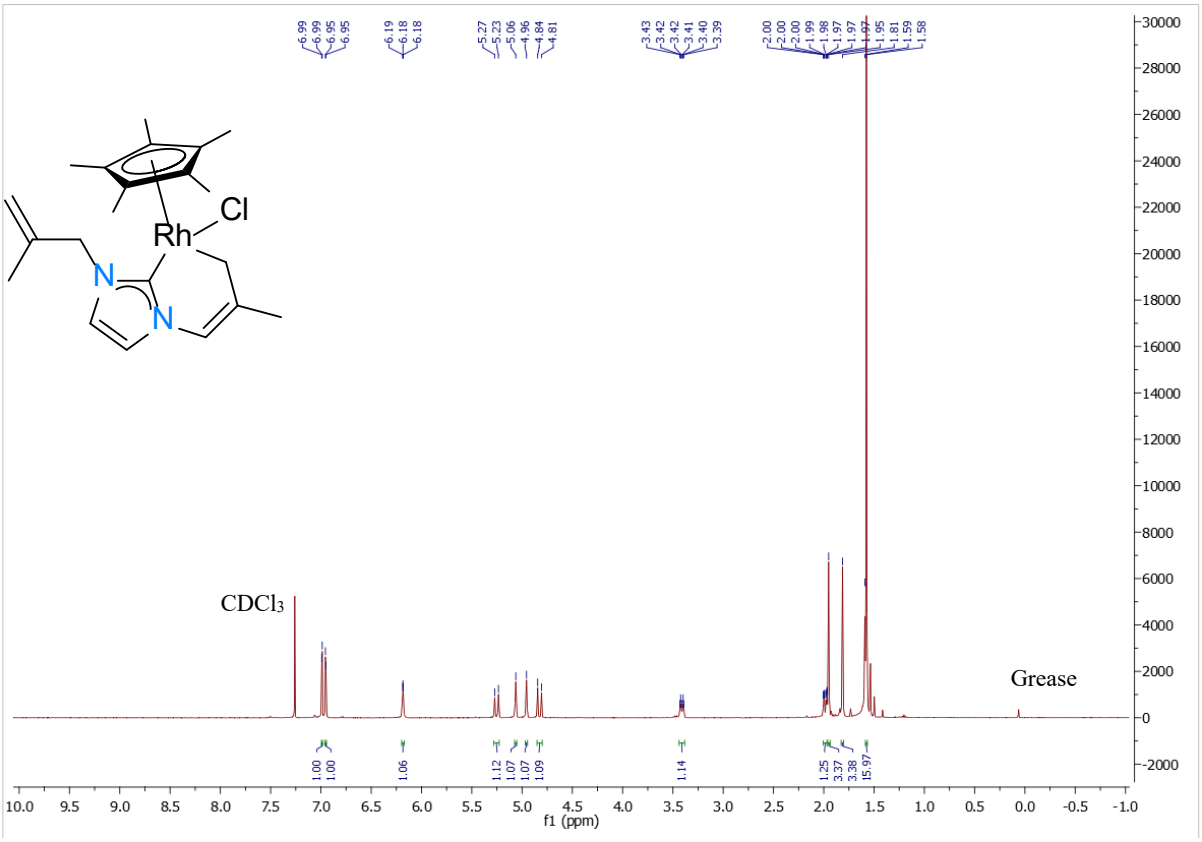

Figure S8 ^{1}H NMR spectrum of complex **2**.

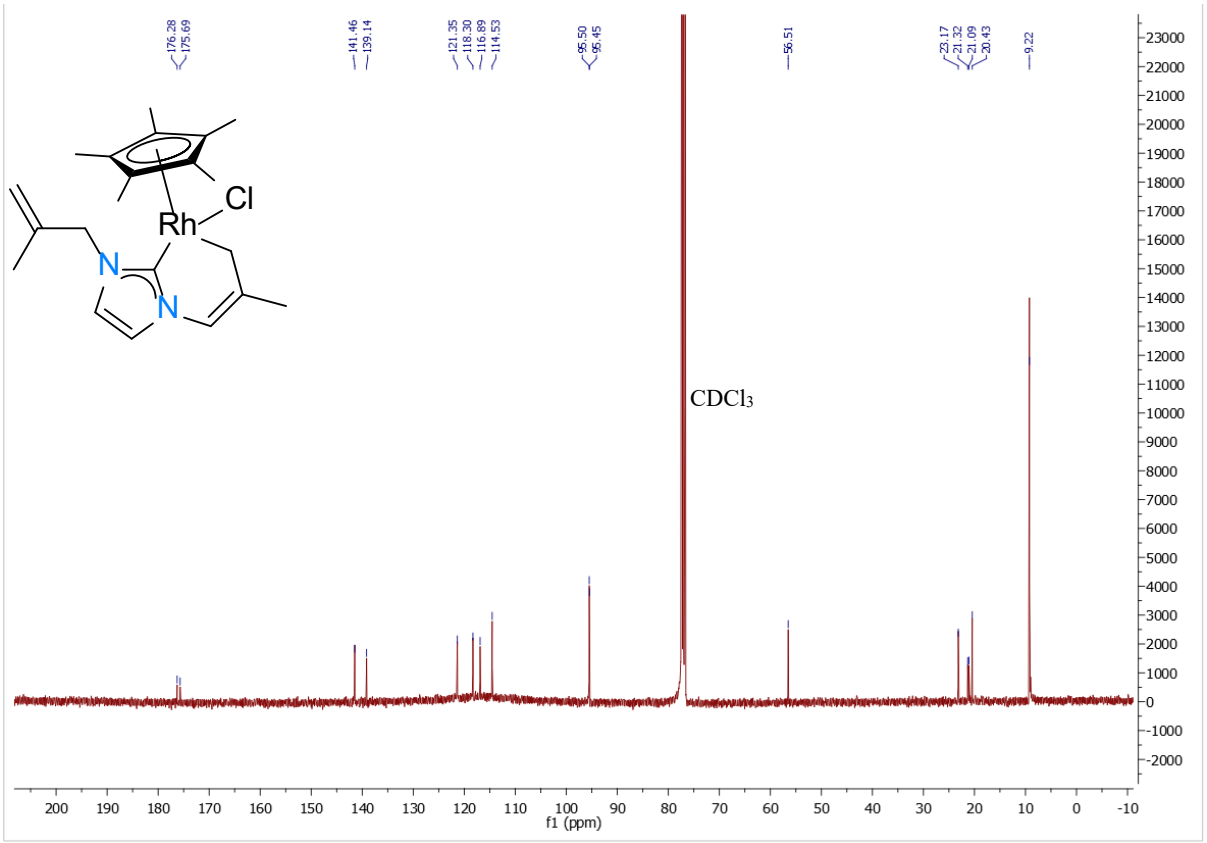

Figure S9 ^{13}C NMR spectrum of complex **2**.

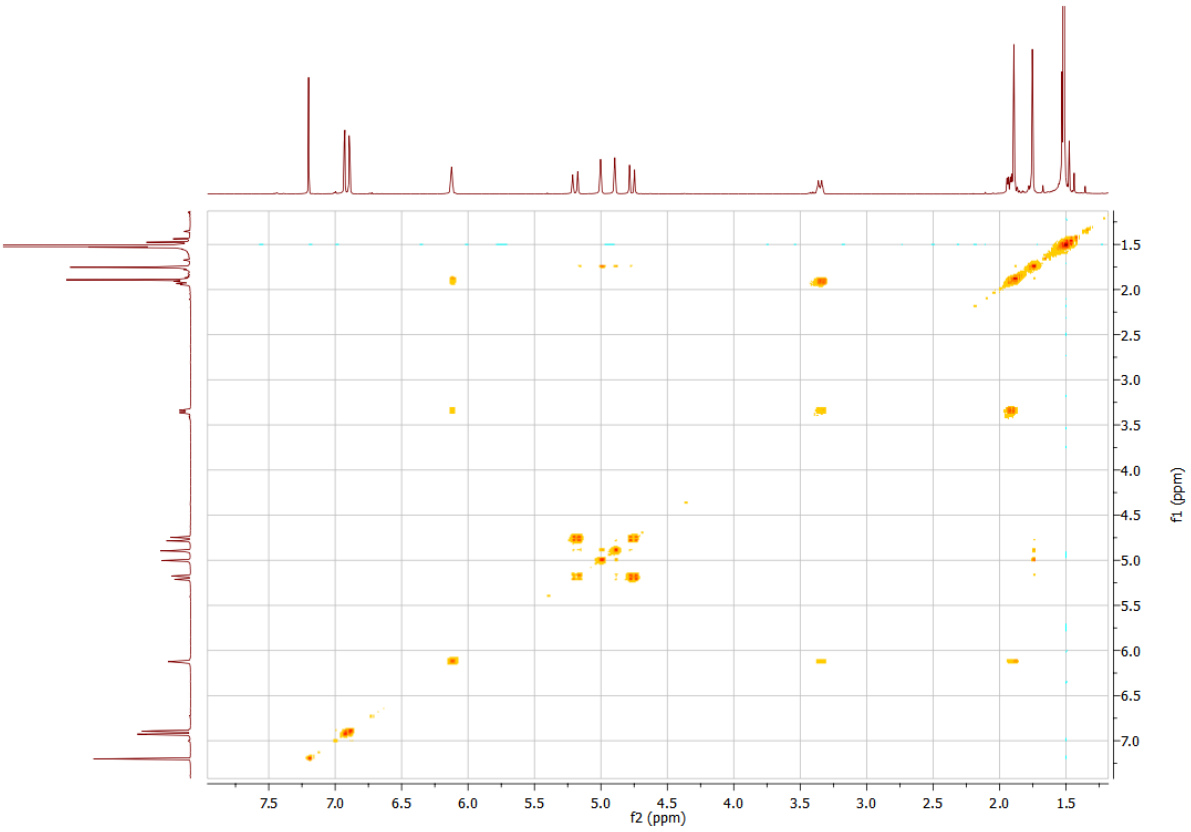

Figure S10 2D-COSY $^{1}H\{^{1}H\}$ NMR spectrum of complex **2**.

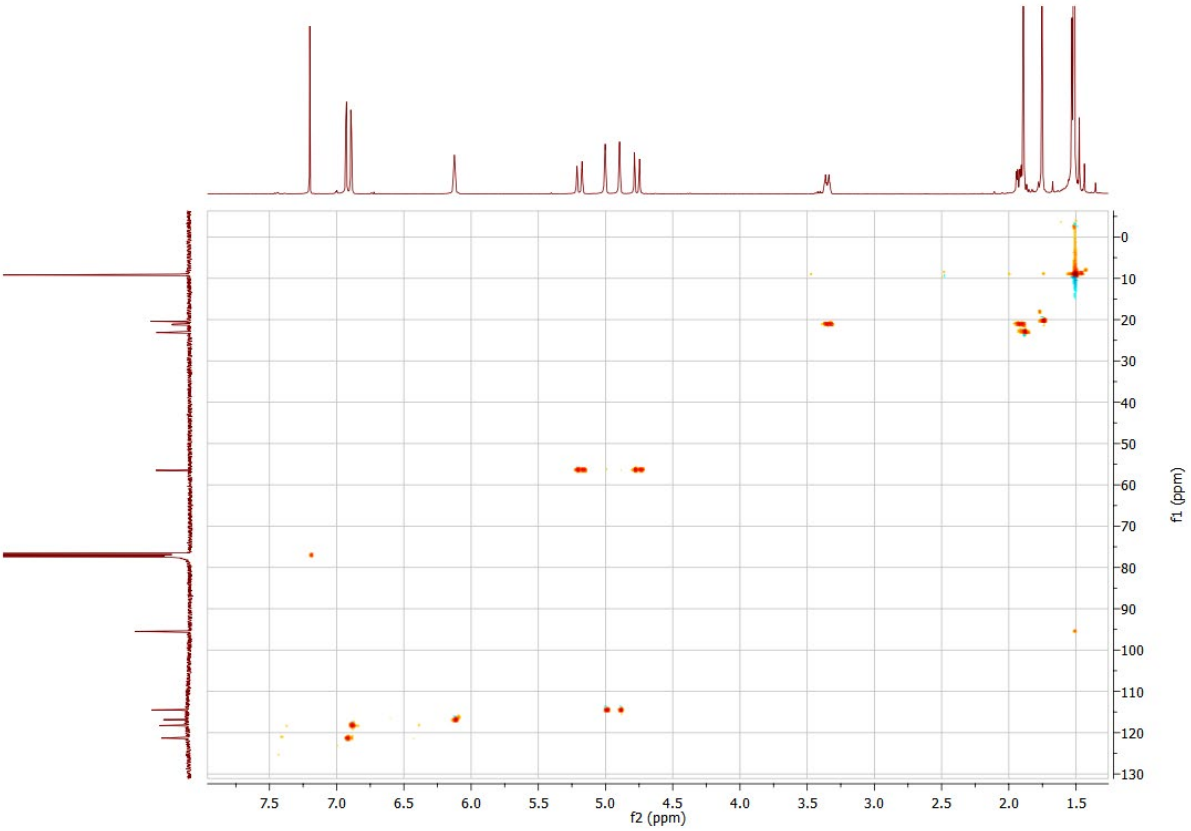

Figure S11 2D-HSQC $^{13}C\{^{1}H\}$ NMR spectrum of complex **2**.

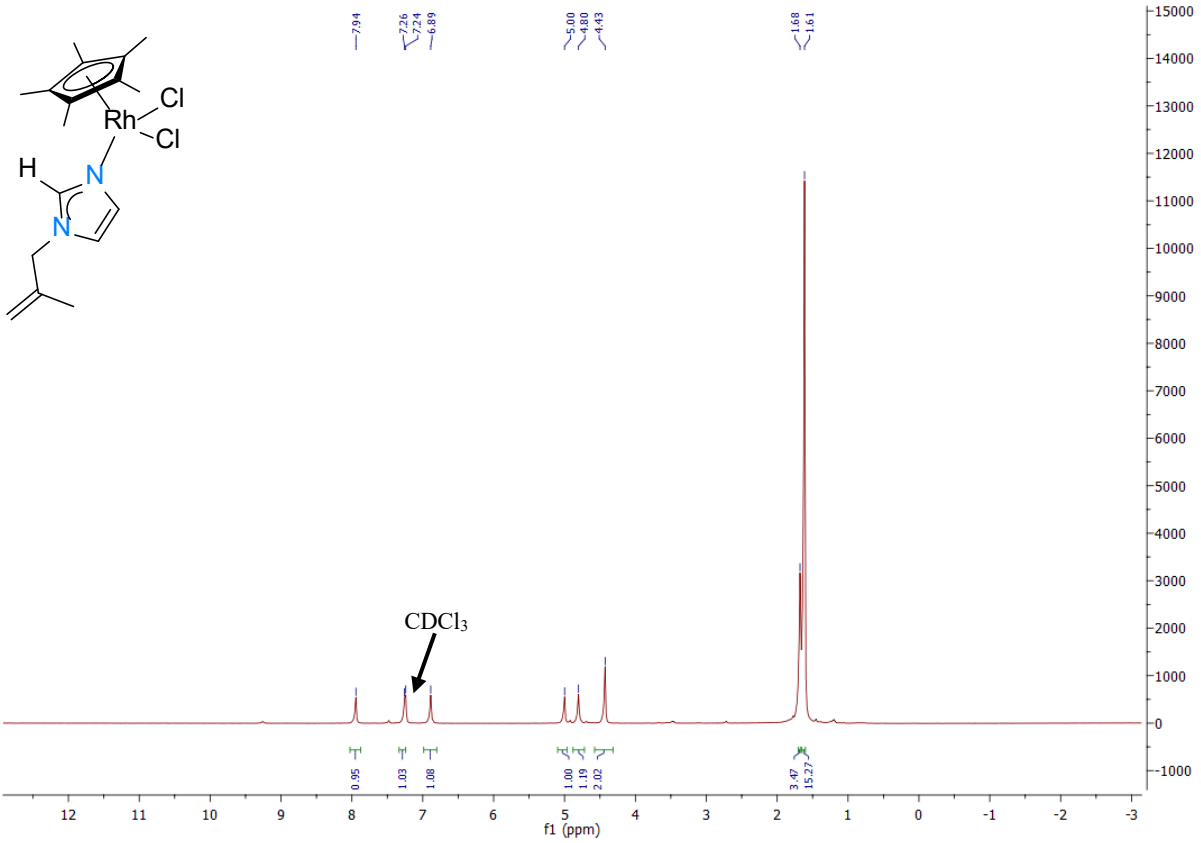

Figure S12 ^{1}H NMR spectrum of complex **2b**.

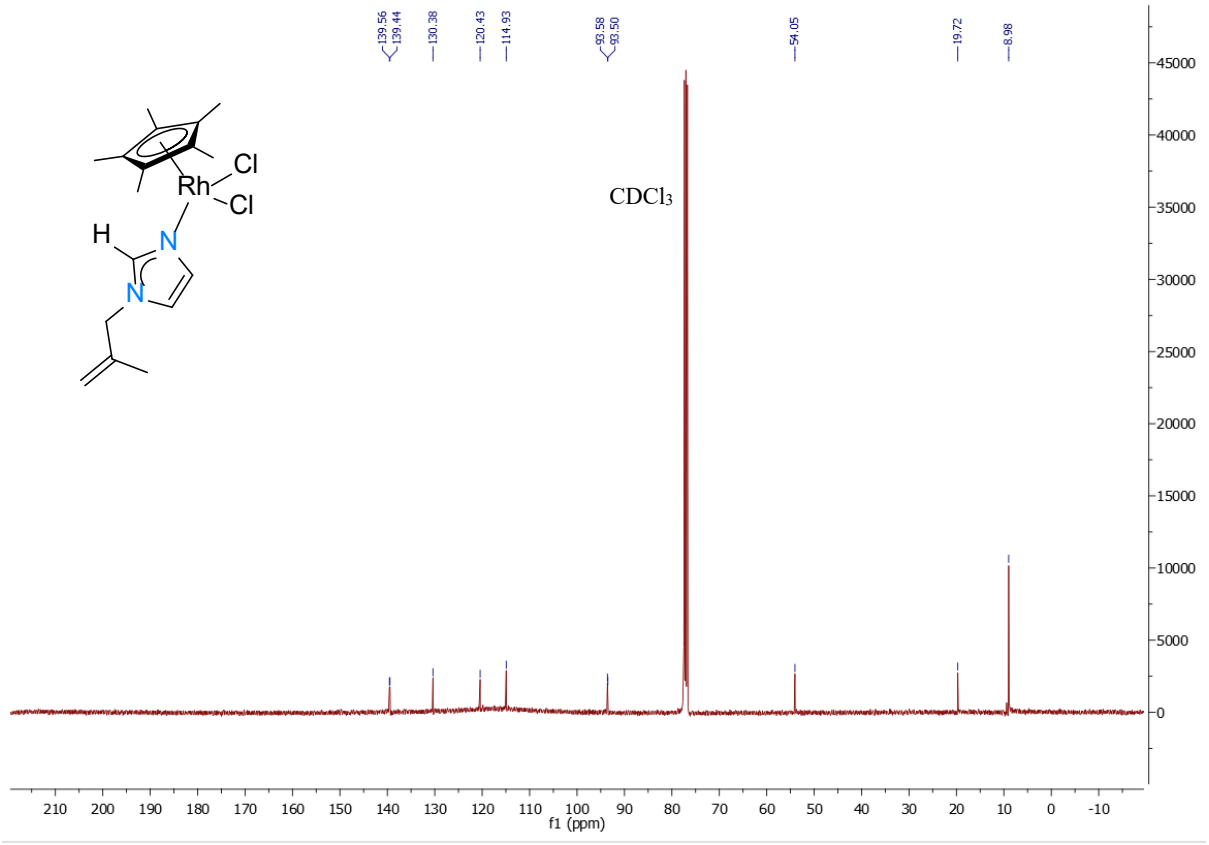

Figure S13 ^{13}C NMR spectrum of complex **2b.**

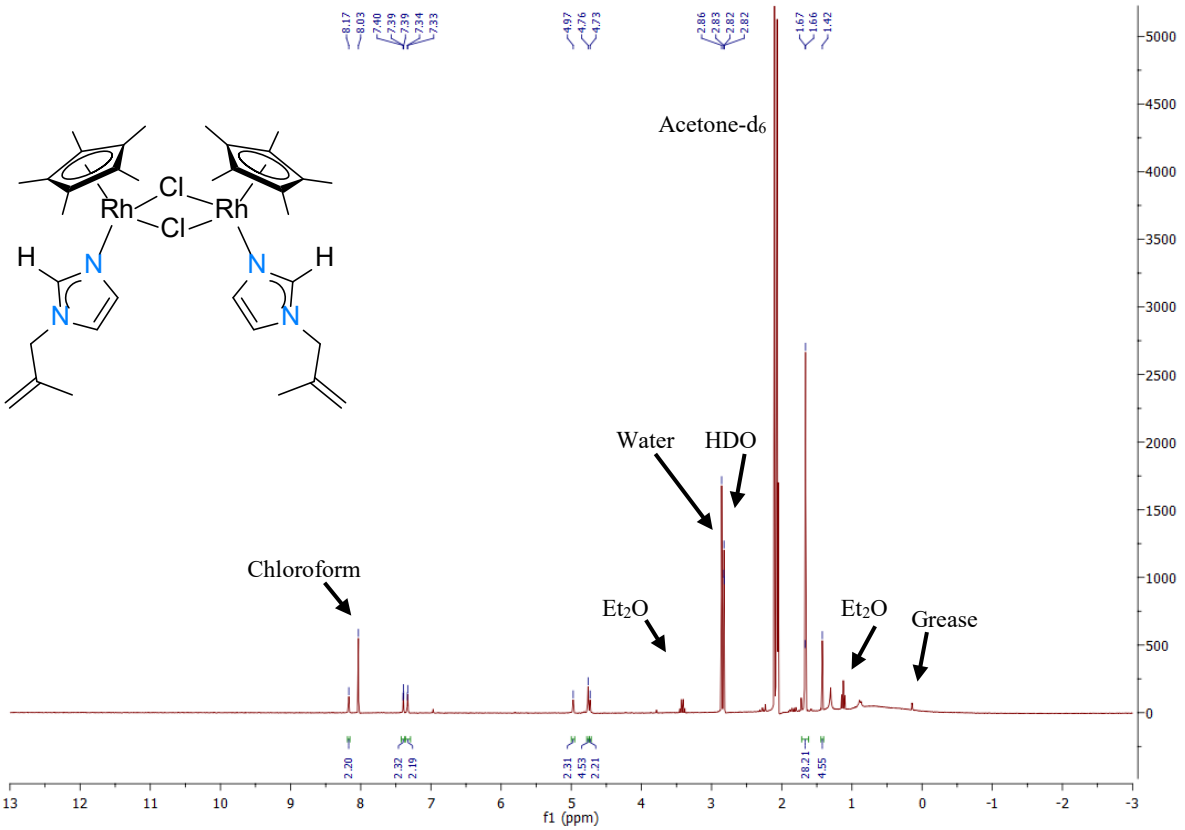

Figure S14 ^{1}H NMR spectrum of complex **2bd**.

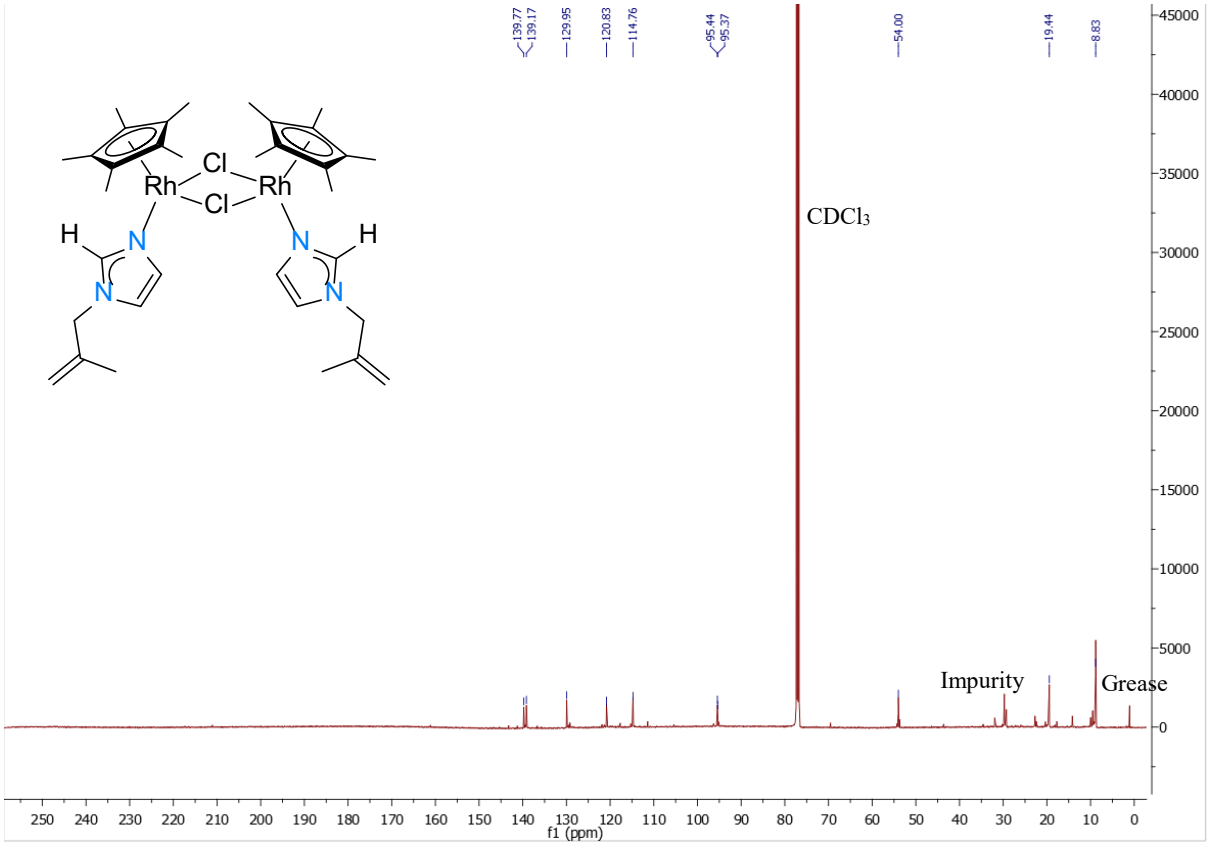

Figure S15 ^{13}C NMR spectrum of complex **2bd**.

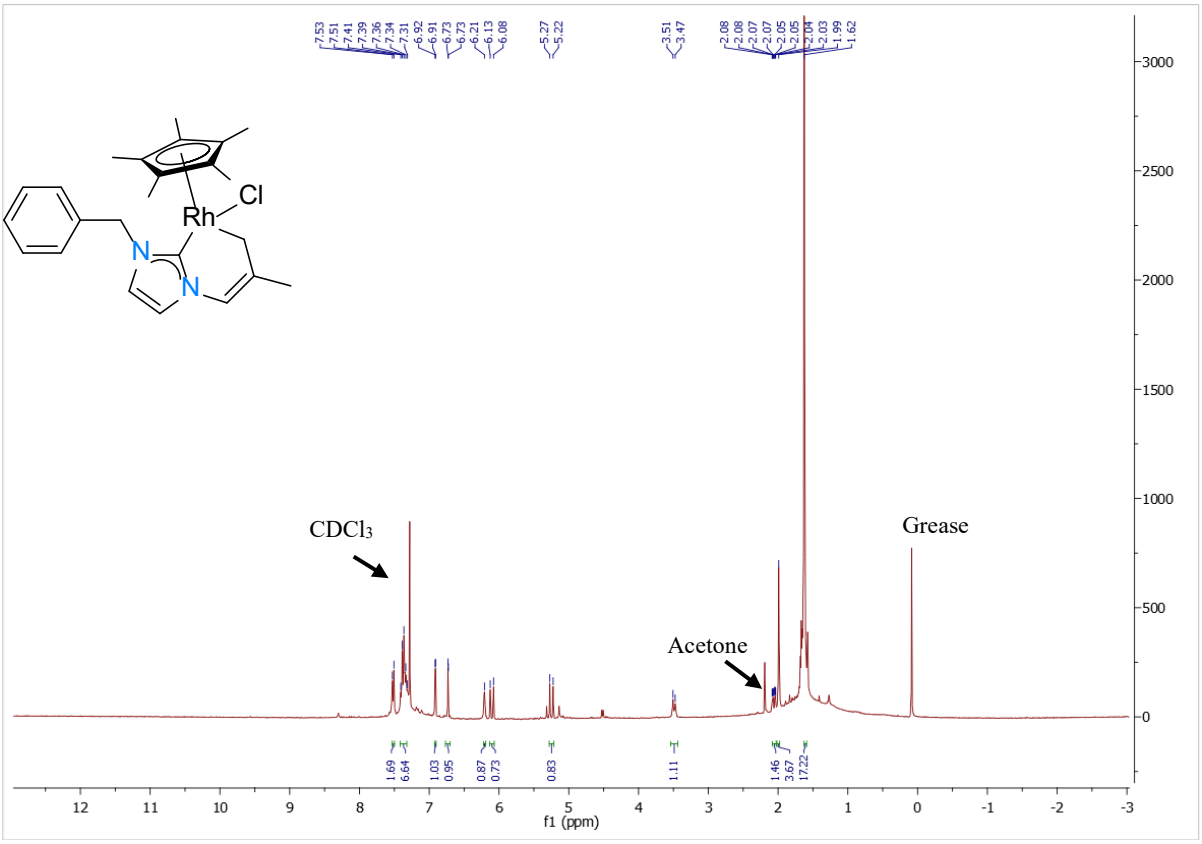

Figure S16 ^{1}H NMR spectrum of complex **3**.

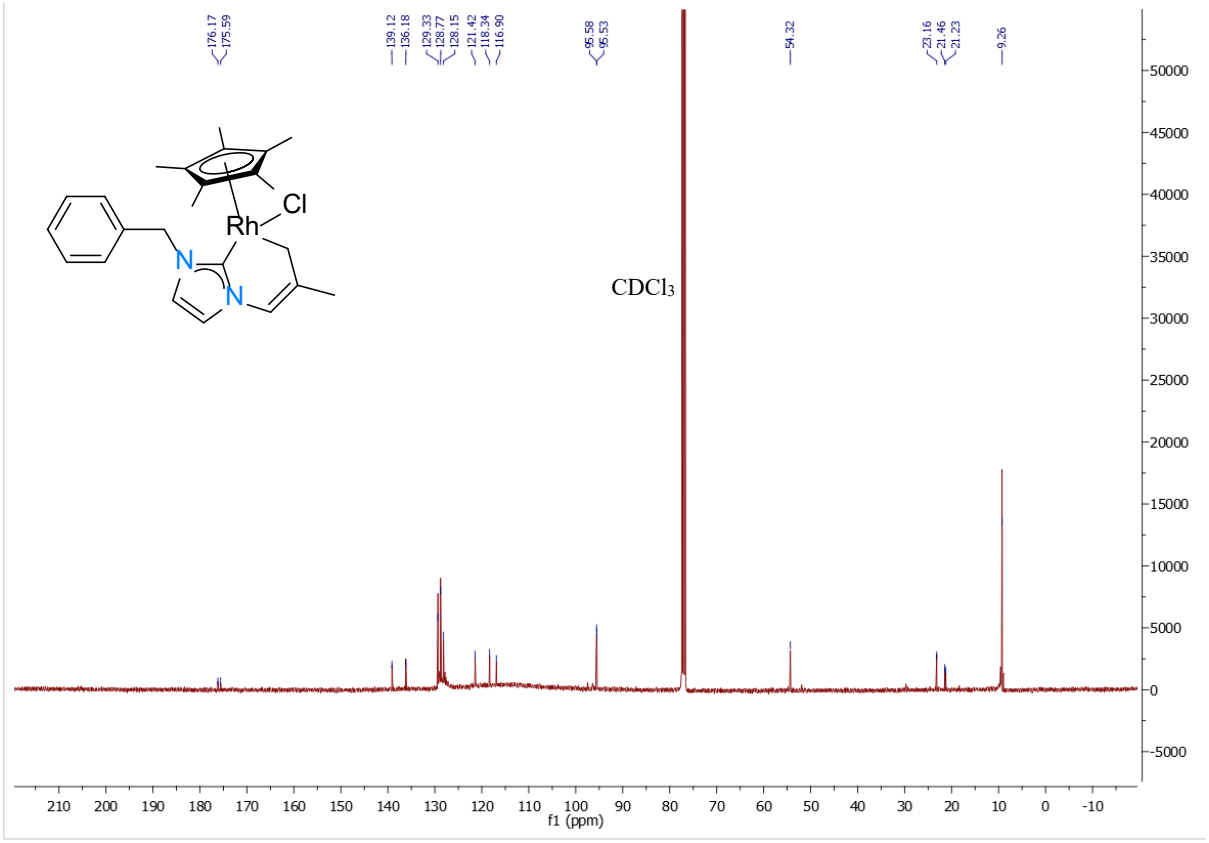

Figure S17 ^{13}C NMR spectrum of complex **3**.

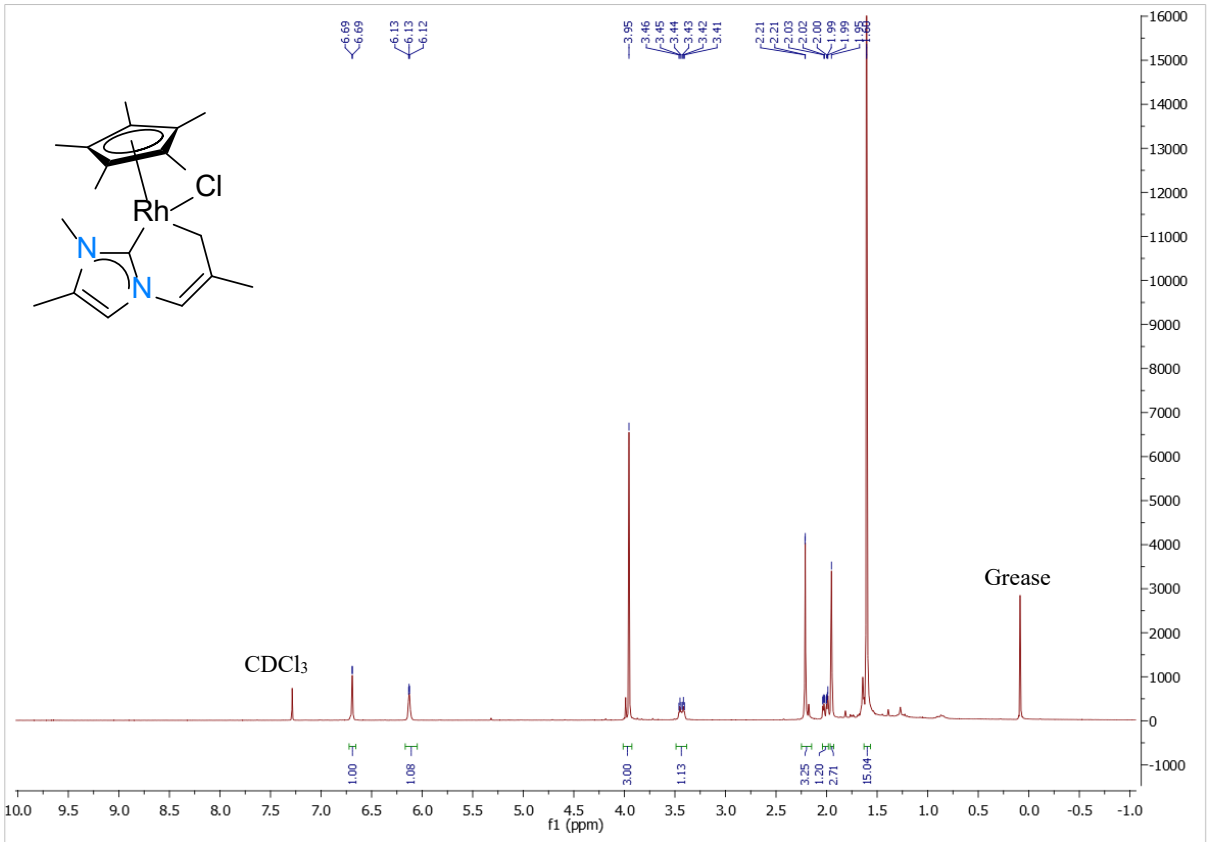

Figure S18 ^{1}H NMR spectrum of complex **4**.

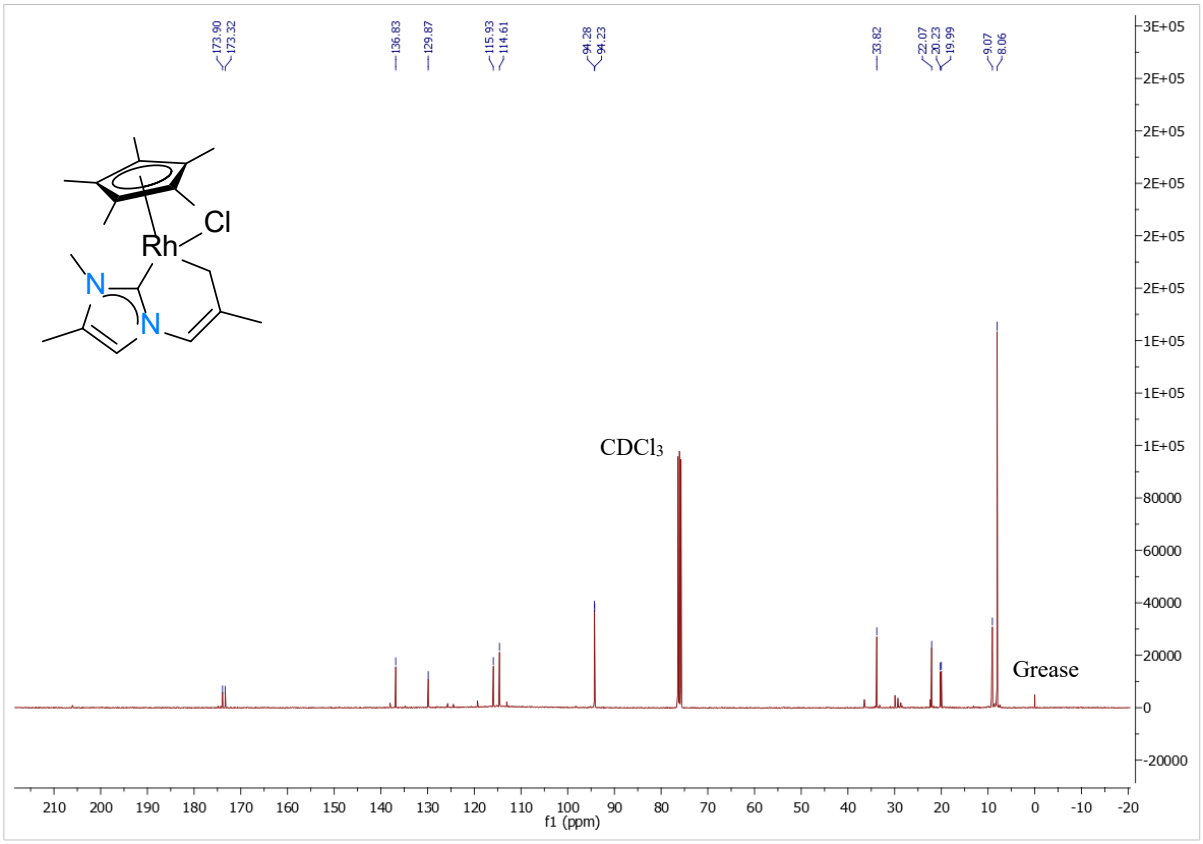

Figure S19 ^{13}C NMR spectrum of complex **4**.

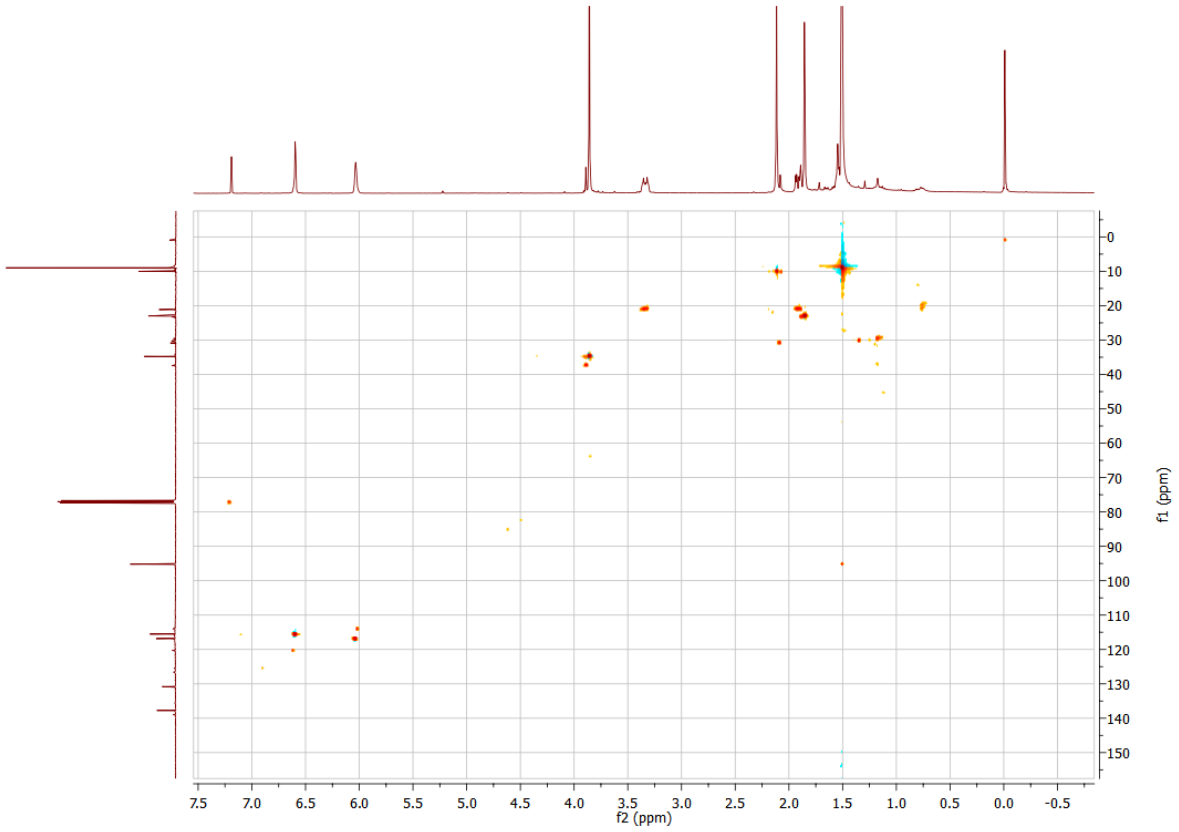

Figure S20 2D-HSQC $^{13}C\{^{1}H\}$ NMR spectrum of complex **4**.

2. ^{1}H NMR spectra of the Ag- and Rh-carbene intermediate species (**Figures S21, S22**).

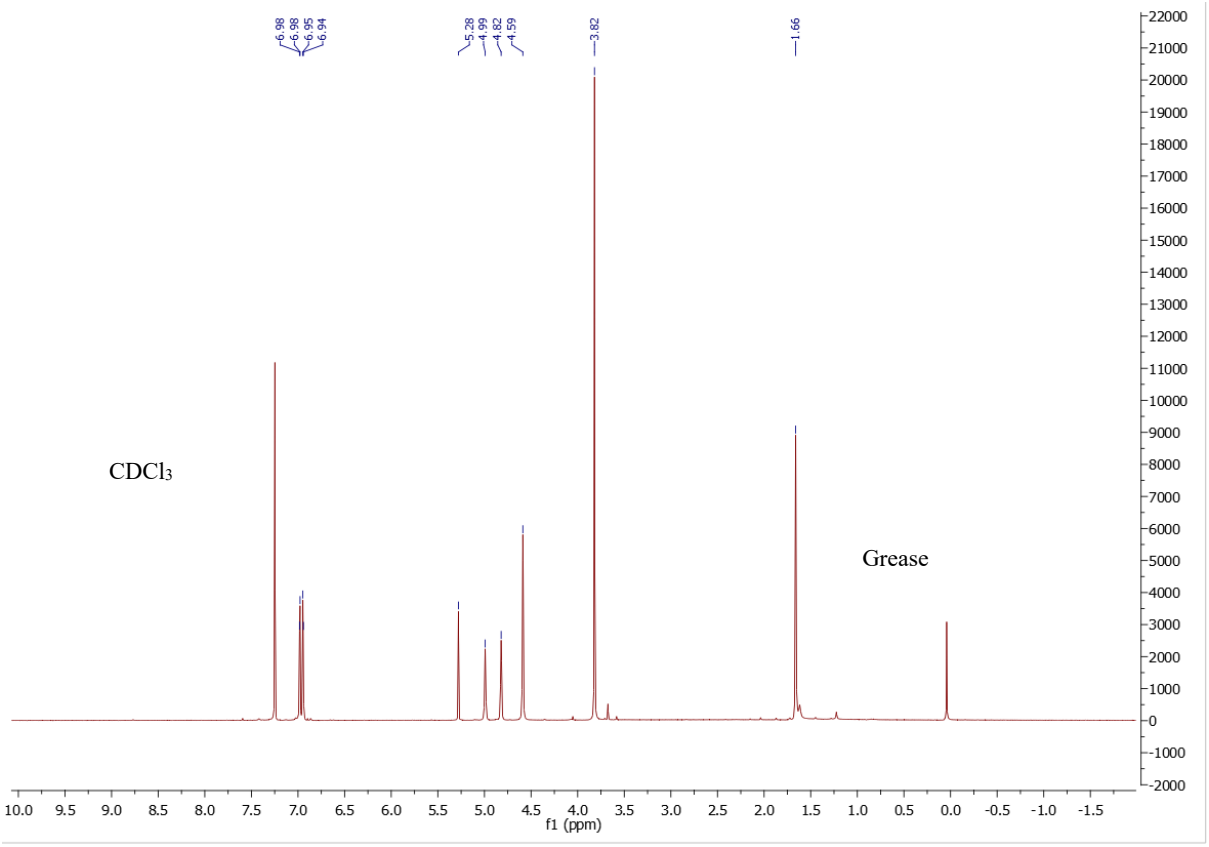

Figure S21 Confirmation of formation of silver carbene species of **L1** after 1 hour of reaction time *via* ^{1}H NMR spectrum.

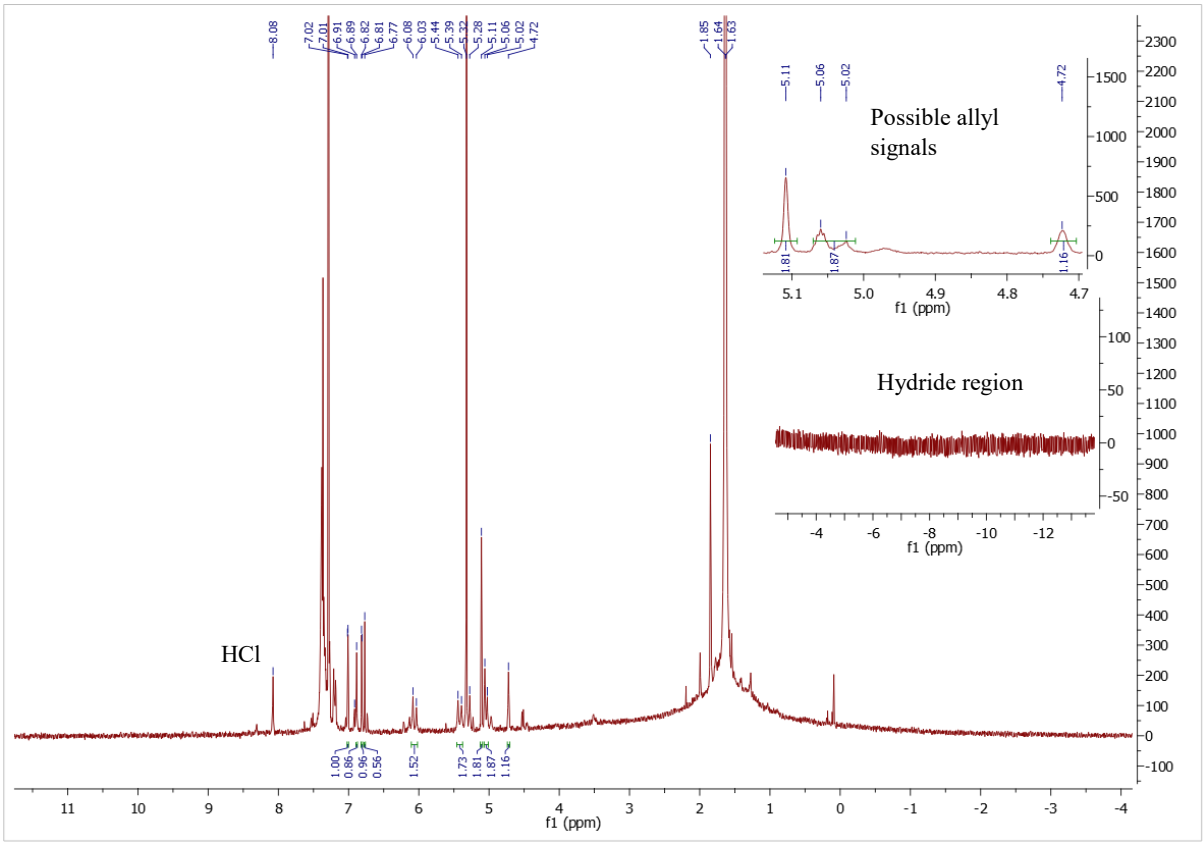

Figure S22 ^{1}H NMR spectrum of the reaction mixture in the formation of **3**.

3. Crystallographic data and structure refinement parameters (**Tables S1-S3**).

Table S1. Crystal data and structure refinement for **L1**, **1**, **1b**, and **1bd**.

Complex	L1	1	1b	1bd
Emp. formula	$C_8H_{15}N_2OCl$	$C_{18}H_{26}N_2ClRh$	$C_{14}H_{21.64}N_2O_{0.32}Cl_2Rh$	$C_{28}H_{42}N_4Cl_2F_{12}P_2Rh_2$
CCDC Identifier	2065431	2065434	2065433	2065432
Form. weight (g.mol^{-1})	190.67	408.77	396.94	1001.32
Crystal system	monoclinic	monoclinic	monoclinic	triclinic
Space group	$P2_1/c$	$P2_1/n$	$P2_1/c$	P-1
Crystal descr.	colourless block	yellow blade	red block	yellow blade
a (Å)	10.1179(3)	8.3947(14)	7.22397(5)	8.37580(10)
b (Å)	10.9871(3)	15.336(3)	14.22202(11)	11.0890(2)
c (Å)	10.4348(3)	14.2730(14)	15.74072(10)	11.49320(10)
α (°)	90	90	90	114.6020(10)
β (°)	118.536(4)	92.234(4)	91.1461(6)	105.0605(10)
γ (°)	90	90	90	93.8590(10)
Volume (Å^3)	1019.08(6)	1836.1(5)	1616.87(2)	918.30(2)
Z	4	4	4	1
Abs. coeff. (m.mm^{-1})	0.334	1.074	11.503	10.242
F(000)	408.0	840.0	805.0	500.0
Independent refl.	2007	4479	3179	3623
Completeness (%)	100	92.4	100	99.9
Data/Restr/Para	2007/0/117	4479/0/206	3179/0/190	3623/0/232
Goodness of fit on F^2	1.064	1.088	1.054	1.064
Final R$_1$ indexes	0.0299	0.0609	0.0509	0.0375
wR$_2$ indices (all data)	0.0764	0.1090	0.1342	0.0931
Largest diffr. peak and hole (e.Å^{-3})	0.23/-0.18	0.64/-0.46	1.42/-1.88	0.86/-1.42

Table S2. Crystal data and structure refinement for **2**, **3**, and **2bd**.

Complex	2	2bd	3	4
Emp. formula	$C_{21}H_{30}N_2ClRh$	$C_{34}H_{50}N_4Cl_2F_{12}P_2Rh_2$	$C_{24}H_{30}N_2ClRh$	$C_{19}H_{29.1}ClN_2O_{0.23}Rh$
CCDC Identifier	2065436	2065437	2065435	2081484
Form. weight (g.mol^{-1})	448.83	1081.44	484.86	427.58
Crystal system	triclinic	monoclinic	monoclinic	triclinic
Space group	*P*-1	$P2_1/c$	$P2_1/c$	*P*-1
Crystal descr.	yellow block	yellow block	yellow block	yellow block
a (Å)	8.87720(10)	11.9494(4)	17.6252(3)	8.3277(2)
b (Å)	9.1631(2)	14.5628(3)	10.55540(10)	8.4664(3)
c (Å)	13.2708(2)	13.5155(5)	12.2784(2)	14.8256(6)
α (°)	109.942(2)	90	90	78.840(4)
β (°)	93.3990(10)	116.157(4)	100.2450(10)	87.889(3)
γ (°)	91.1110(10)	90	90	69.605(3)
Volume (Å^3)	1012.07(3)	2111.06(13)	2247.87(6)	960.70(6)
Z	2	2	4	2
Abs. coeff. (m.mm^{-1})	0.982	8.962	7.307	8.470
F(000)	464	1088.0	1000.0	442.0
Independent refl.	3975	4155	4421	3783
Completeness (%)	99.9	99.8	99.9	99.9
Data/Restr/Para	3975/0/233	4155/0/260	4421/0/259	3783/0/231
Goodness of fit on F^2	1.059	1.190	1.109	1.117
Final R_1 indexes	0.0201	0.0363	0.0467	0.0560
wR_2 indices (all data)	0.0520	0.1027	0.1340	0.1557
Largest diffr. peak and hole (e.Å^{-3})	0.41/-0.58	0.97/-0.54	2.67/-1.15	1.42/-0.96

Table S3. Selected bond lengths and angles for **L1**, **1-3**, **1b**, **1bd**, and **2bd**.

Description	L1	1	1b	1bd	2	2bd	3	4
Cp*$_{cent}$-Rh1[a]	-	1.861(3)	1.776(3)	1.767(3)	1.860(3)	1.762(3)	1.862(3)	1.863(8)
Rh1-Cl1	-	2.4219(14)	2.4401(9)	2.4622(9)	2.4260(4)	2.4430(10)	2.4239(10)	2.4206(16)
Rh1-Cl2	-	-	2.4119(9)	2.4382(9)	-	2.4480(10)	-	-
Rh1-C2	-	1.990(5)	-	-	2.0045(16)	-	2.010(4)	2.015(6)
Rh1-C7	-	2.095(6)	-	-	2.0898(16)	-	2.098(4)	2.100(6)
Rh1-N2	-	-	2.107(3)	2.099(3)	-	2.102(3)	-	-
C6-C7	1.3190(19)	1.476(8)	-	-	1.485(2)	-	1.483(6)	1.470(9)
C6-C8	1.4981(18)	1.502(8)	-	-	1.504(2)	-	1.506(7)	1.516(10)
C6-C5	1.5042(18)	1.302(8)	-	-	1.334(3)	-	1.341(6)	1.311(10)
N2-C5	1.4657(16)	1.412(7)	-	-	1.420(2)	-	1.420(6)	1.431(9)
Rh1-C7-C6	-	115.0(4)	-	-	115.57(11)	-	114.9(3)	116.0(4)
C7-C6-C8	123.61(13)	118.1(6)	-	-	117.52(6)	-	119.0(4)	118.0(6)
C5-C6-C7	123.47(12)	121.8(6)	-	-	122.21(16)	-	122.3(4)	123.7(6)
N2-C5-C6	113.61(10)	123.0(5)	-	-	121.19(15)	-	121.4(4)	121.7(6)
C2-Rh1-C7	-	81.6(2)	-	-	82.69(7)	-	82.70(16)	83.2(3)
Cl1-Rh1-Cl2	-	-	89.96(4)	83.90(3)	-	85.16(3)	-	-
Cl1-Rh1-N2	-	-	88.32(8)	88.66(10)	-	88.28(10)	-	-
Cl1-Rh1-C2	-	94.13(14)	-	-	91.00(5)	-	95.47(12)	92.69(19)
Cl1-Rh1-C7	-	88.28(16)	-	-	87.24(5)	-	88.70(12)	89.31(19)
Rh1-C7-C6-C5	-	48.0(8)	-	-	-48.4(2)	-	47.0(5)	-45.1(8)
C7-C6-C5-N2	5.49(19)	-3.3(10)	-	-	3.6(3)	-	-2.7(7)	3.6(10)
Rh1-C2-N2-C5	-	-8.1(7)	-	-	0.7(2)	-	-6.1(6)	8.7(9)
C2-N2-C5-C6	99.89(15)	-20.4(9)	-	-	23.8(3)	-	-21.5(7)	18.0(10)
N2-C5-C6-C8	167.72(12)	178.1(6)	-	-	-178.75(17)	-	178.1(4)	-177.5(6)
Rh1-N2-C2-N1	-	-	-167.8(3)	172.7(3)	-	-164.4(3)	-	-
Rh1-N2-C4-C3	-	-	167.6(3)	-173.5(3)	-	-164.4(4)	-	-

[a] Cp*$_{cent}$ = centroid of Cp* ligand.

4. ^{1}H NMR spectra of catalysis reaction mixtures obtained in C_6D_6

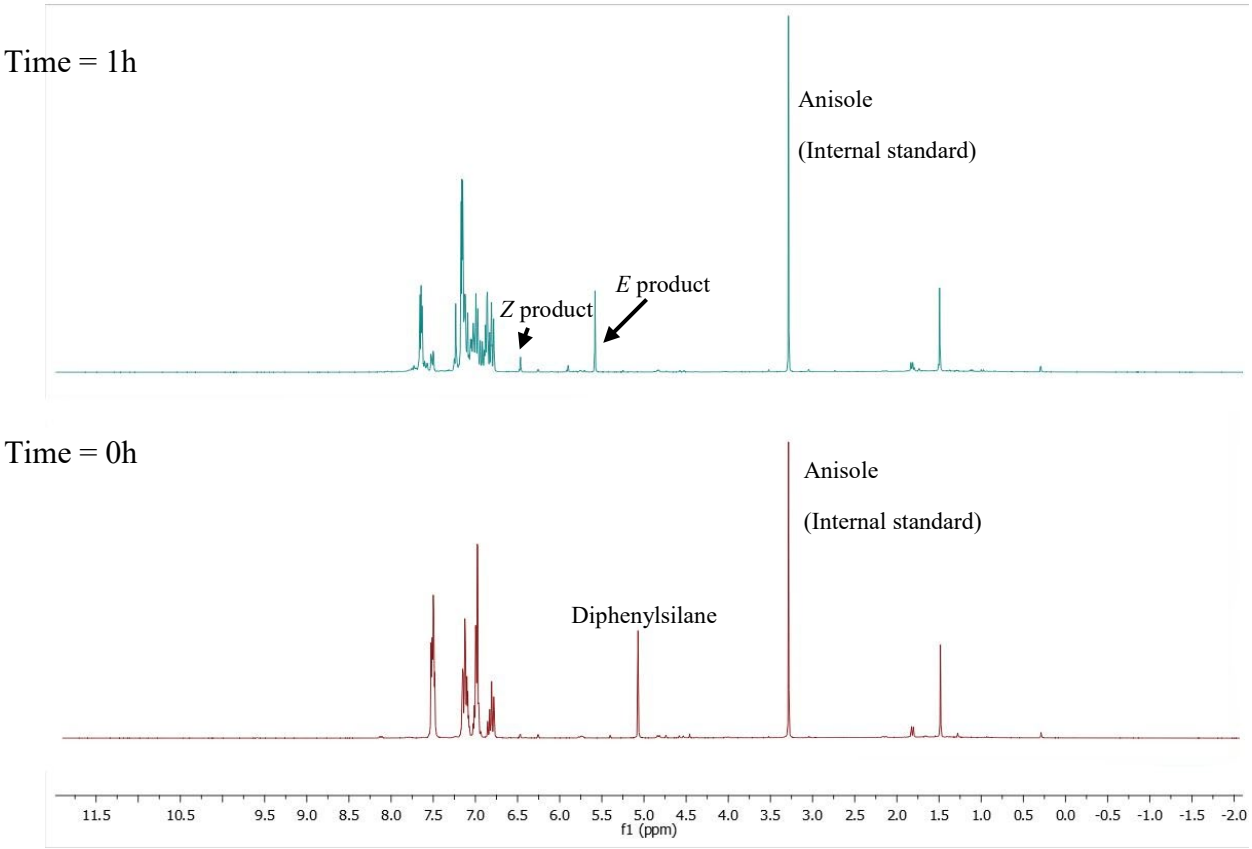

Figure S23 ^{1}H NMR spectrum of catalysis reaction mixture obtained in C_6D_6. General reaction conditions: PhCCPh (18 mg, 0.1 mmol), H_2SiPh_2 (11 µL, 0.1 mmol), Complex **2** (4 mol%), anisole (10 µl, 0.11 mmol), C_6D_6, 80 °C, 1 hour.

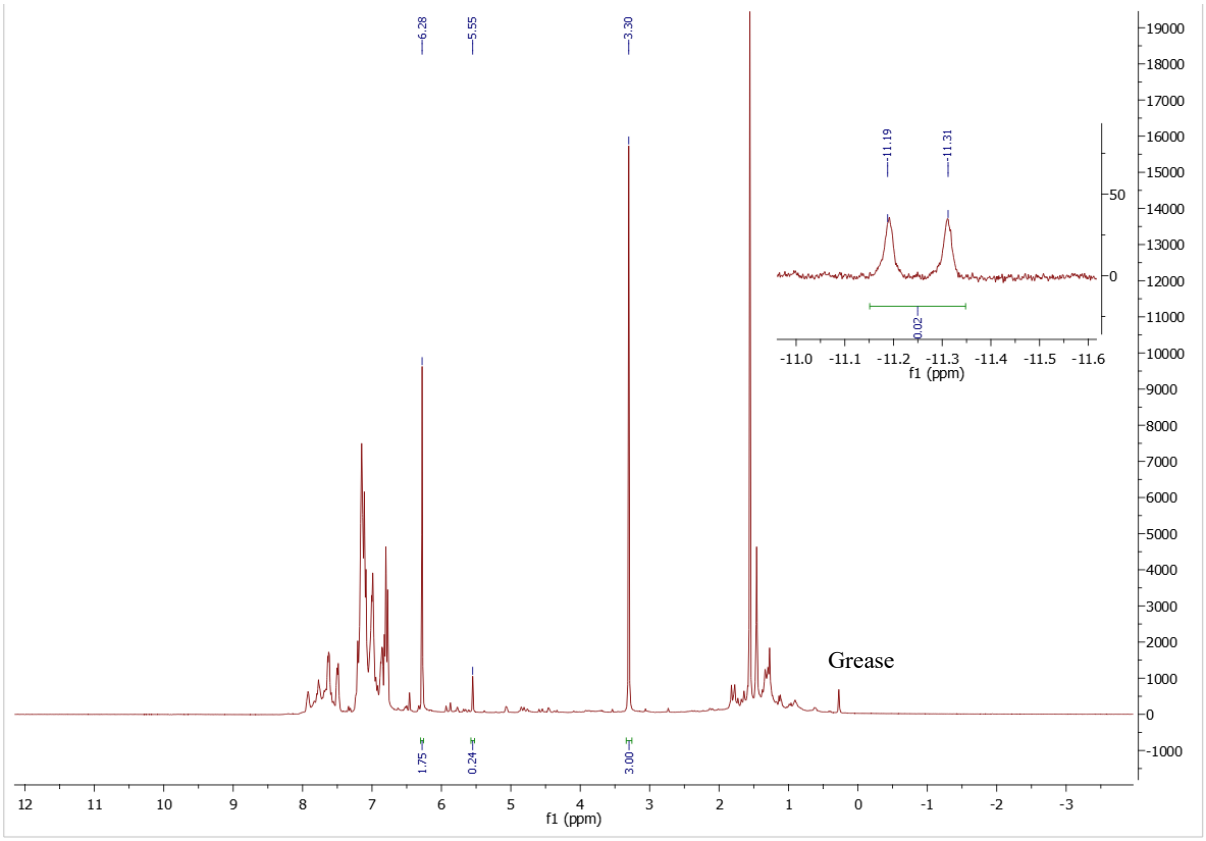

Figure S24 Complex **2** with H_2SiPh_2 and diphenylacetylene in a 1:1:1 ratio to observe Rh-H formation after 10 mins of reaction time. General reaction conditions: PhCCPh (18 mg, 0.1 mmol), H_2SiPh_2 (11 µL, 0.1 mmol), **2** (0.1 mmol), anisole (10 µl, 0.11 mmol), C_6D_6, 80 °C. Isomer assignment was based on literature reports.[1]

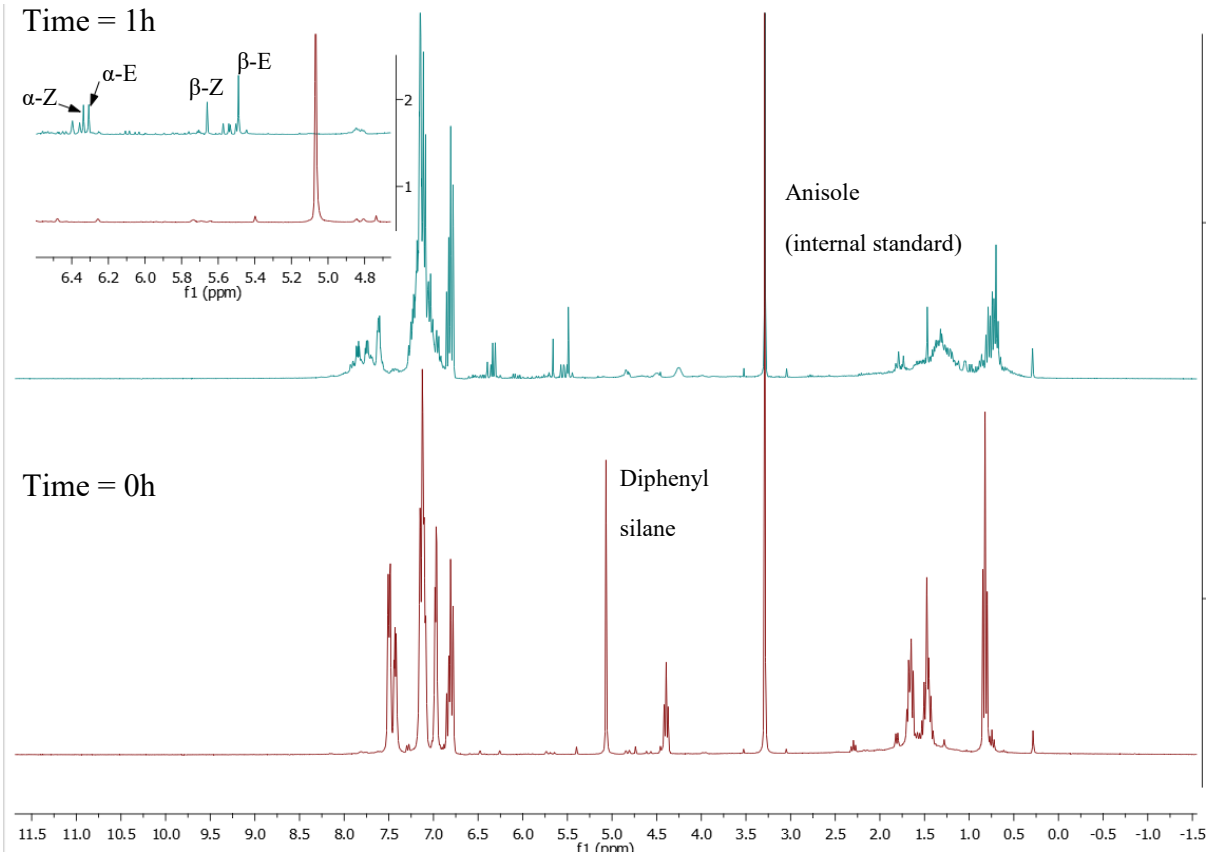

Figure S25 ^{1}H NMR spectrum of hydrosilylation of 1-phenylhex-1-yn-3-ol (**Table 2**, entry 7) obtained in C_6D_6. General reaction conditions: 1-phenylhex-1-yn-3-ol (19 µl, 0.1 mmol), H_2SiPh_2 (11 µL, 0.1 mmol), Complex **2** (4 mol%), anisole (10 µl, 0.11 mmol), C6D6, 80 °C, 1 hour. Integration was done against the internal standard (anisole) to determine the conversion, yield and selectivity of catalysed reaction. Isomer assignment was based on literature reports.[1]

5. Conversion versus time plot using **2** (**Figure S26**).

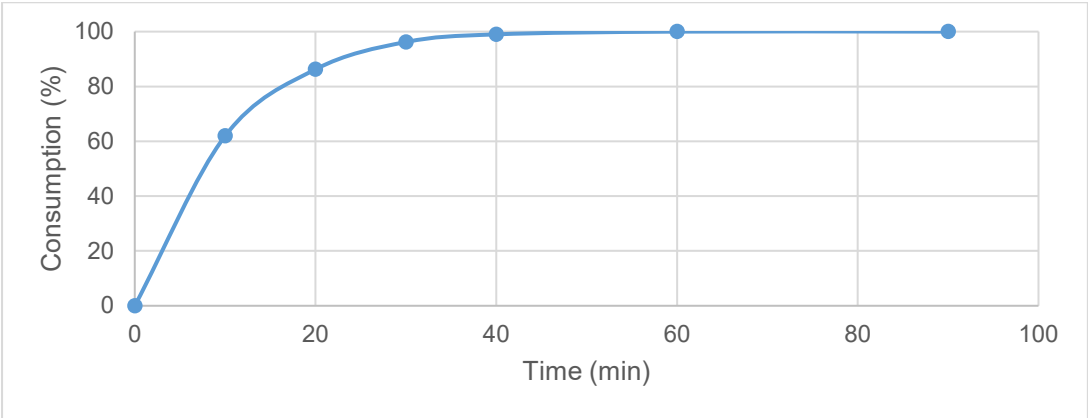

Figure S26. Conversion versus time plot in the hydrosilylation of diphenylacetylene at 80°C utilising **2**. General reaction conditions: PhCCPh (18 mg, 0.1 mmol), H_2SiPh_2 (11 µL, 0.1 mmol), Rh catalyst (4 mol%), anisole (10 µl, 0.11 mmol), C_6D_6, 80 °C, 1 hour.

6. Proposed mechanism for the catalytic hydrosilylation of alkynes using the N-bound Rh complexes as pre-catalysts.

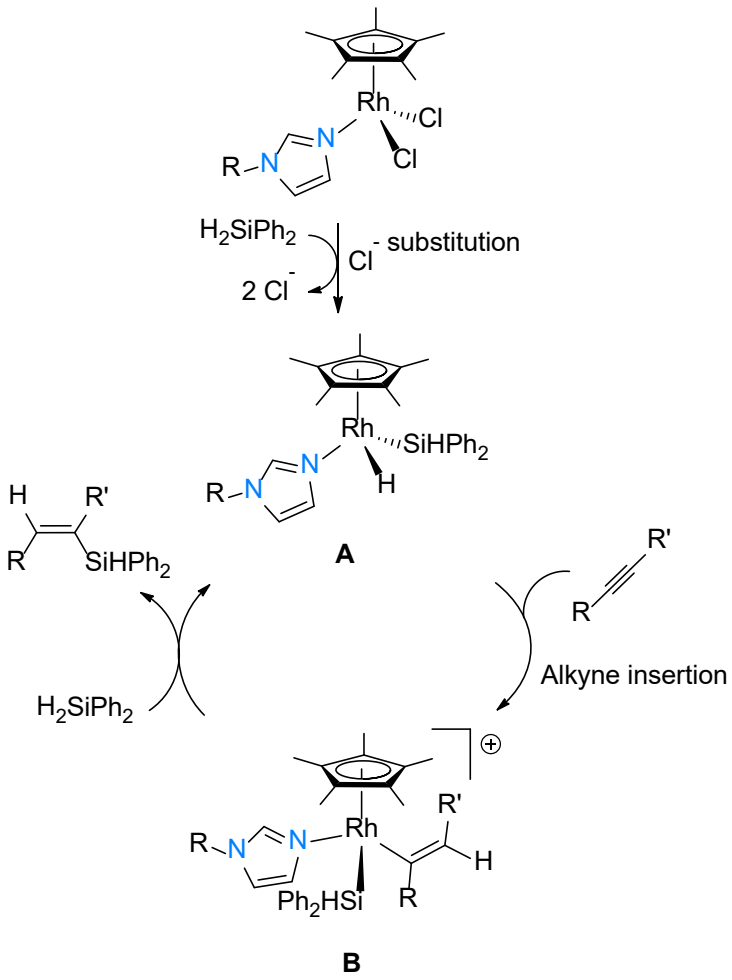

Scheme S1. Proposed catalytic cycle for the catalytic hydrosilylation of internal alkynes using N-bound Rh complexes as catalysts.

References

1. (a) Teo, W. J.; Wang, C.; Tan, Y. W.; Ge, S., Cobalt-catalyzed Z-selective hydrosilylation of terminal alkynes. *Angew. Chem., Int. Ed.* **2017,** *56* (15), 4328-4332; (b) Li, R. H.; Zhang, G. L.; Dong, J. X.; Li, D. C.; Yang, Y.; Pan, Y. M.; Tang, H. T.; Chen, L.; Zhan, Z. P., Xantphos Doped POPs-PPh_3 as Heterogeneous Ligand for Cobalt-Catalyzed Highly Regio-and Stereoselective Hydrosilylation of Alkynes. *Chem. - Asian J.* **2019,** *14* (1), 149-154.